Random Delay Induced Resonance in Duffing Oscillator

L. Ravisankar,[1] V. Ravichandran,[1] V. Chinnathambi,[1,*] and S. Rajasekar[2,†]

[1] *Department of Physics, Sri K.G.S. Arts College, Srivaikuntam 628 619, Tamilnadu, India*

[2] *School of Physics, Bharathidasan University, Tiruchirapalli 620 024, Tamilnadu, India*

Abstract

We consider the ubiquitous Duffing oscillator driven by a weak periodic force with a time-delay linear feedback term. For a random time-delay we numerically explore the effect of strength of feedback term (γ) and standard deviation σ of Gaussian white noise type delay time on resonance. We show the occurrence of single and double resonance and bring out the mechanisms associated with the resonances.

Keywords: random delay, resonance, Duffing oscillator

*Electronic address: `veerchinnathambi@gmail.com`

†Electronic address: `rajasekar@cnld.bdu.ac.in`

I INTRODUCTION

Nonlinear oscillators are capable of displaying variety of resonances depending on the nature of perturbations. Some of the interesting resonances are nonlinear resonance [1, 2] (the perturbation is an external periodic force), Coherence resonance [3, 4] (induced by noise in the absence of an external periodic force), stochastic resonance [5, 6] (induced by noise in the presence of an external periodic force), ghost resonance [7, 8] (resonance at a missing fundamental frequency of the multi-frequency force), vibrational resonance [9, 10] (resonance at a low-frequency force induced by a high-frequency force) and chaos resonance [11] (due to a chaotic perturbation). In recent years great interest has been focused on time-delayed nonlinear dynamical systems and many fascinating dynamics have been observed [12, 13]. The time-delay can be a single constant, multiple constants, continuous over a range, state-dependent, distributive, periodically varying with time and random. The present paper is concerned with stochastic and vibrational resonance with random time-delay.

In certain conditions the time-delay can be random. For example, in biochemical reactions, a source of time-delay can be the response time of the last step which can be random due to the molecular thermal motion. In population dynamics when the time-delay due to the gestation or incubation times depend on the variations of the external environment and living conditions due to climate and weather changes then it has to be treated as a random one [14, 15]. Random delay enters in the immune response models if the outbreak of a disease caused by an infection are due to complicated biological and environmental processes [16]. Random delay is found to give rise stabilization of steady state and periodic orbits [17–21], synchronization [22, 23], H-infinity filtering [24, 25], state estimation [26], existence of a stationary random solution [27], controlling of systems [28] and bifurcations [29] have been studied in certain systems with random delays. Random delay induced resonance with and without an external periodic force is realized in the Langevin equation [30, 31]. Solutions of certain linear differential equations with random delay have been analyzed in ref. [32].

The goal of the present paper is to study the occurrence of resonance with random delay-time. We choose the reference model system as the under damped Duffing oscillator with linear time-delayed feedback and driven by an external weak periodic force. First we show that typical stochastic resonance occurs in the system with additive Gaussian white noise when the time-delay τ is a constant. Next we show the resonance occurs in the absence of

additive Gaussian white noise but with the time-delay τ being Gaussian. We consider the effect of γ, the strength of the feedback term and σ the standard deviation of the Gaussian noise representing the time-delay τ. Single and double resonances are found when γ or σ is varied. We explain the mechanisms of the resonance using time series plot and phase portrait.

II RESONANCE WITH FIXED TIME-DELAY

The equation of motion of the ubiquitous Duffing Oscillator with a linear time - delayed feedback, driven by a periodic force of frequency ω and additive noise η is given by

$$\ddot{x} + d\,\dot{x} + \omega_0^2 x_i + \beta x_i^3 + \gamma x(t-\tau) = f\ \cos\ (\omega t + \eta(t)) \tag{1}$$

$\eta(t)$ is a Gaussian white noise with mean zero and standard deviation σ. τ is the time-delay and γ is the strength of the feedback. Throughout our study we fix the values of the parameters as $d = 0.5, \omega_0^2 = 1, \beta = 1, f = 0.1$ and $\gamma = 0.1$. The potential of the system is a double-well form with a local maximum at $x = 0$ and two local minima at $x_\pm = \sqrt{\mid \omega_0^2 \mid / \beta}$. Euler method with step size $h = 0.001$ is used to numerically integrate the eq.(1). Before investigating the effect of random time-delay in the absence of $\eta(t)$, first we consider the system (1) with constant time-delay. We fix $\tau = 0.5$ and numerically integrate eq.(1). After leaving the solution corresponding to first 500 drive cycles as a transient, we calculate the response amplitude Q over next 30,000 drive cycles. Q is given by

$$Q = \frac{\sqrt{Q_\mathrm{S}^2 + Q_\mathrm{C}^2}}{f}\ . \tag{2a}$$

with

$$Q_\mathrm{S} \;=\; \frac{2}{nT}\int_0^{nT} x(t)\sin(2\pi t/T)\,\mathrm{d}t\ , \tag{2b}$$

$$Q_\mathrm{C} \;=\; \frac{2}{nT}\int_0^{nT} x(t)\cos(2\pi t/T)\,\mathrm{d}t\ , \tag{2c}$$

where $T = 2\pi/\omega$ and $= 30000$. Figure 1 presents the numerically computed Q as a function of the parameter σ (characterizing the strength of noise) for two values of ω. This figure shows a typical noise-induced resonance curve. For both $\omega = 0.1$ and $\omega = 1$ as the value of σ increases from a small value Q increases, reaches a maximum value at a critical value of

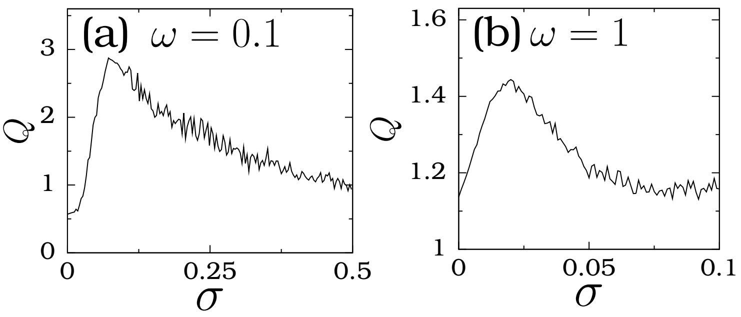

FIG. 1: Variation of the response amplitude Q with the standard deviation of the noise $\eta(t)$ for the system (1) for (a) $\omega = 0.1$ and (b) $\omega = 1$. The values of the parameters in the system (1) are $d = 0.5, \omega_0^2 = -1, \beta = 1, f = 0.1, \tau = 0.5$ and $\gamma = 0.1$.

σ and then slowly decreases. For $\omega = 0.1$, Q is maximum at $\sigma = 0.067$ while for $\omega = 1$, Q is maximum at $\sigma = 0.021$.

The dynamics of the system is different at resonances for $\omega = 0.1$ and 1. In fig.2 the evolution of the state variable x is plotted for four values of σ for $\psi = 0.1$. In fig.2a for $\sigma = 0.001$, $x(t)$ is confined to the region $x > 0$ (there is another trajectory bounded to the interval $x < 0$). $x(t)$ is similar to the input periodic signal, however, it is perturbed by the noise term. At a critical value of σ noise-induced switching between the regions $x < 0$and $x > 0$ occurs. This is shown in fig.2b for $\sigma = 0.04$. The time intervals between successive switchings are not the same. Switching intervals are random. At another critical value of $\sigma (= 0.067)$ almost periodic switching between the two wells occurs. This is the case in fig.2c. The mean residence time of a trajectory in each of the two potential wells is $\approx T/2$ where $T = 2\pi/\omega$. For $\sigma >> 0.06$ rapid switching of the trajectories between the regions $x > 0$ and $x < 0$ happens (fig.2d). Figure 3 displays $x(t)$ versus t for $\omega = 1$ and $\sigma = 0.021$. Though the response amplitude Q becomes a maximum at $\sigma = 0.021$ there is no periodic switching of the trajectory between the two wells. This example shows that periodic switching is not necessary at stochastic resonance.

III RESONANCE WITH RANDOM TIME-DELAY

Next, consider the system (1) without the additive noise term but treat the delay time τ as random. Particularly choose it as a Gaussian white noise with mean zero and variance

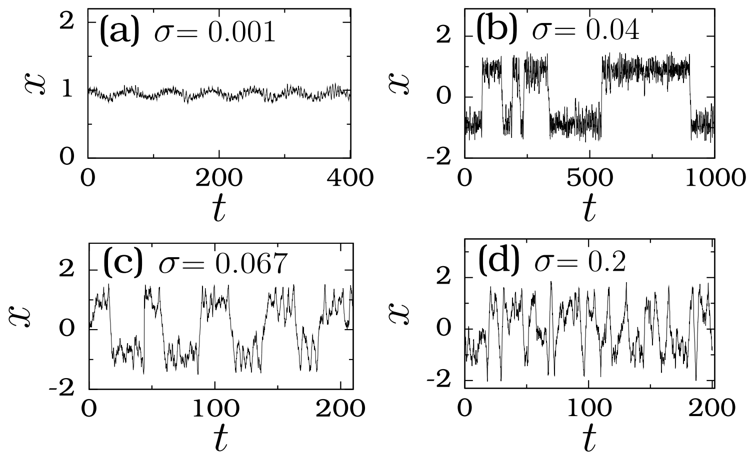

FIG. 2: $x(t)$ versus t of the system-1 for four values of σ with $\omega = 0.1$.

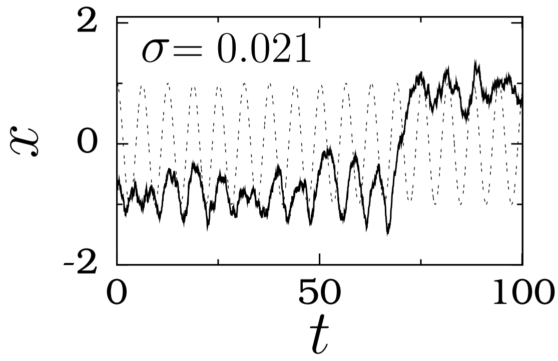

FIG. 3: $x(t)$ versus t of the system-1 for $\sigma = 0.021$ and $\omega = 1$. The dashed line is the rescaled input signal $f \cos \omega t$.

σ^2. Because a Gaussian random number can be a negative the feedback term is chosen as $x(t- \mid \tau \mid)$. The equation of motion of the system is

$$\ddot{x} + d\,\dot{x} + \omega_0^2 x_i + \beta x_i^3 + \gamma x(t- \mid \tau \mid) = f\ \cos\ (\omega t) \tag{3}$$

We treat the strength of the feedback described by the parameter γ as the control parameter. Figure 4 presents the dependence of the response amplitude Q on γ and σ when $\omega = 0.1$, for a range of fixed values of $\sigma(0 < \sigma < 3)$ a single resonance when γ is varied (fig.4a). The value of Q at resonance decreases with increase in the value of σ. Q at resonance becomes relatively much for $\sigma > 1.75$. As shown in fig.4b a different behavior takes place for $\omega = 1$. For each fixed value of σ there are two resonances when is varied from, say -1. The second

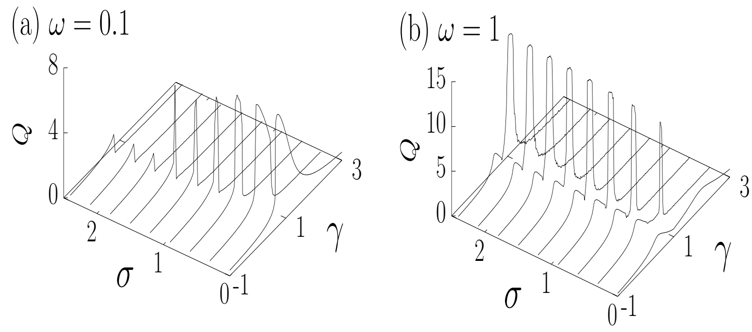

FIG. 4: Q versus σ and γ for two fixed values of ω of the system (2) with $d = 0.5, \omega_0^2 = -1, \beta = 1$, and $f = 0.1$.

resonance is the dominant resonance.

In fig.5 we plot γ_R, the value of γ at which resonance occurs and Q_{max}, the value of Q at $\gamma = \gamma_R$, as a function of σ for $\omega = 1$. The value of γ at which first resonance occurs (denoted by γ_R^1) and the corresponding value of Q (denoted as $Q_{max}^{(1)}$) are almost constant with the parameter σ of the random time delay. γ_R^2 sharply decreases with σ and then increases almost in a linear fashion. In fig.5b $Q_{max}^{(2)}$ displays sinusoidal type variation. $Q_{max}^{(2)}$ increase rapidly with σ and then attains a saturation.

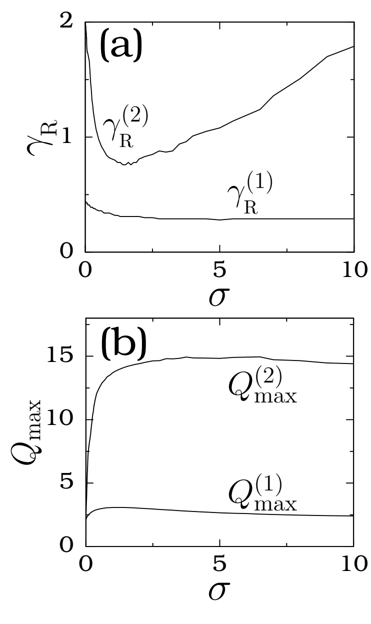

FIG. 5: The variations of (a) γ_R (the value of γ at which resonance takes place) and (b) Q_{max} ($\gamma = \gamma_R$) as a function of the parameter σ associated with the randomness of the time delay.

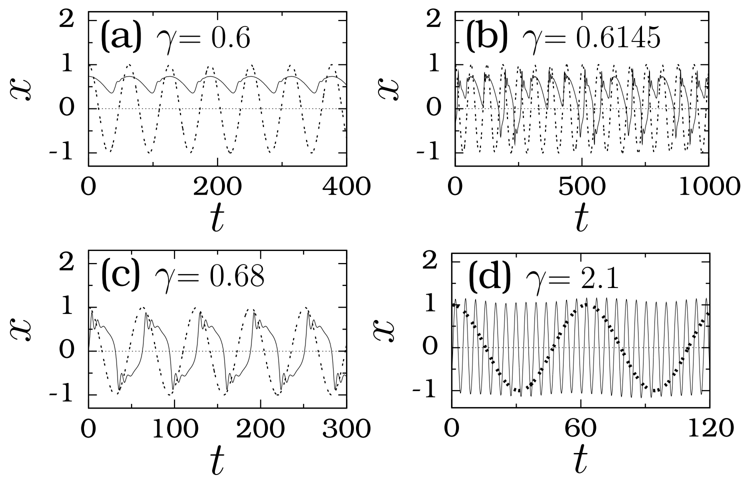

FIG. 6: $x(t)$ versus t of the system-2 for four values of γ when $\omega = 0.1$ and $\sigma = 0.1$. The dotted curve is the rescaled $f \cos \omega t$ and continuous curve is the numerically computed $x(t)$.

We understand the mechanism of observed stochastic resonance using trajectory plot. Figure 6 shows evolution of $x(t)$ for four fixed values of γ and for $\sigma = 0.1$ and $\omega = 0.1$. For this value of ω the resonance occurs at $\gamma = 0.6$. In all the subplots of fig.6 the dotted line is the rescaled input periodic signal $f \cos \omega t$. In fig.6a ($\gamma = 0.6$) far before resonance $x(t)$ is bounded in the region $x > 0$ and is almost periodic with the period of the input periodic force. For $\gamma = 0.6145$ (fig.6b) $x(t)$ switches between the positive and negative values, that is, jumps between the two wells of the double-well potential. The motion is nonperiodic at the time intervals between consecutive jumpings are random. In fig.6c corresponding to the resonance case ($\gamma = 0.68$) the solution $x(t)$ appears almost periodic and we clearly notice cross-well motion and synchronization between $x(t)$ and $f \cos \omega t$ (the external driving force). Compare fig.6c with fig.2c when the resonance is induced by the additive Gaussian white noise. In both the cases the mean residence time is $T/2$, however, in the additive noise induced resonance case $x(t)$ is not periodic. The erratic switching between the wells seen in fig.2d is not observed for $\beta >> 0.68$ in the random delay. The number of switching between the wells per drive period increases with increase in γ (mean residence time in a well decreases with γ), however, the motion is not highly random.

For $\omega = 1$ as shown in fig.4b there are two resonances when γ is varied. The two resonances occur at $\gamma = 0.41$ and 1.72. Now we account these two resonances. Figure 7a displays phase portrait of the system for four values of γ for $\sigma = 0.1$ and $\omega = 1$. As γ

increases from zero the center of the orbit moves towards the origin as the amplitude of the orbit increases. For $\sigma = 0.41$ the amplitude is maximum however the orbit is confined to a single well alone. As the value σ increased further from 0.41 the amplitude of the orbit decreases and the center of the orbit further moves toward the origin. At $\gamma = 1$ the response amplitude Q becomes maximum and the center of the orbit becomes the origin. For $\gamma > 1$ the center of the orbit remains the same while the amplitude Q shows nonmonotonic variation. At $\gamma = 1.72$ Q becomes maximum. This is the second resonance. For $\gamma > 1.72$ the response amplitude decreases. The above scenario around the second resonance is presented in fig.7b. The figs 7a and 7b clearly bring out the differences between the mechanisms of random delay induced two resonances. For sufficiently small ω, for example $\omega = 0.1$ (fig.6), the observed random time-delayed feedback induced resonance is similar to the typical stochastic resonance induced by an additive Gaussian white noise. Here the resonance is due to the almost periodic switching of the trajectories between the two wells. For large ω, for example $\omega = 1$(fig.7) induced double resonance is like the vibrational double - resonance observed in underdamped monostable and bistable oscillators induced by a biharmonic force [9,10]. There is no periodic switching between the potential wells at resonance. In the random delayed system (2) we can introduce an effective potential due to the inclusion of random delayed feedback term. Then as introduced in ref. [9,10] we can define resonant frequency ω_r which depends on the parameters γ and σ in addition to ω_0^2 and β. As γ or σ varies ω_r also vary nonmonotonically so that when ω_r matches with the frequency ω, Q becomes maximum and a resonance results.

Resonance is found when the parameter σ is varied. For $\omega = 1$ and for $\gamma = 0.4$ and 0.65 the response amplitude Q is computed for a range of values of σ and is shown in fig.8. For $\gamma = 0.4$ single resonance at $\sigma = 0.68$ is observed. When $\gamma = 0.65$ Q is maximum at $\sigma = 0.2$ and 2.65. Resonance at these values of σ is also not associated with periodic switching between the potential wells. In fig.9 phase portrait of the system (2) is shown for three values of σ for $\gamma = 0.4$. For all the values of σ the center of the orbit is around $\sqrt{\mid \omega_0^2 0 + \gamma \mid / \beta} \approx 0.775$. The orbit corresponding to $\sigma = 10$ lies in between the orbits of the cases $\gamma = 0.1$ and 0.68. That is, the orbit is not continuously expanding. It expands upto $\gamma = 0.68$ and then shrinks with further increase in γ. We can expect $\omega_r \approx \omega$ at $\gamma = 0.68$.

In fig.10 phase portraits for four values of σ with $\gamma = 0.65$ are plotted. For $\sigma < 0.22$ as σ increases from a small value the center of the orbits remain the same while the size of the

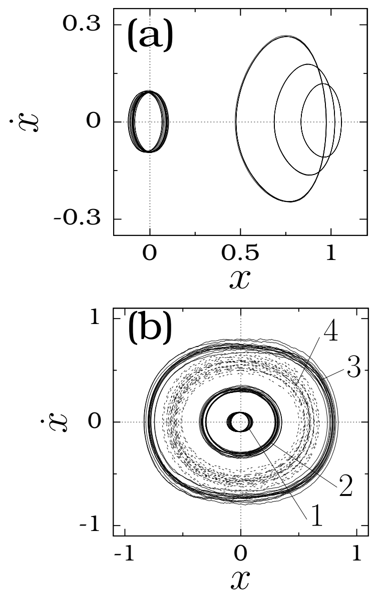

FIG. 7: $x(t)$ versus t of the system (2) with $\omega = 1$ and $\sigma = 0.1$ and for four values of γ around (a) first resonance and second resonance. In (a) the values of γ for the orbits from right to left are $0.1, 0.25, 0.41$ (resonance case) and 1 (at which Q is maximum). In (b) the values of γ for the orbits $1, -4$ are $1, 1.7, 1.72$ (resonance case) and 2 respectively.

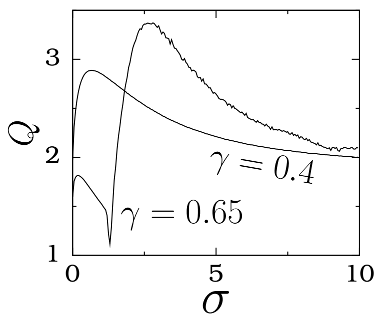

FIG. 8: Variation of the response amplitude Q with the standard deviation of the noise $\eta(t)$ for the system (2) for two values of $\gamma = 0.1$ and $\gamma = 0.65$. The values of the parameters in system (2) are $d = 0.5, \omega_0^2 = -1, \beta = 1, f = 0.1$, and $\tau = 0.5$.

orbit (and the value of Q) increases and becomes maximum at $\sigma = 0.2$ (first resonance value) and then decreases. At $\sigma = 1.22$ onset of cross-well motion occurs. This is shown in fig.10b for $\sigma = 1.25$. At $\sigma = 2.65$ Q becomes a maximum (second resonance). In fig.10 we can clearly notice difference between the orbits shown in fig.10c and those shown in figs 10b

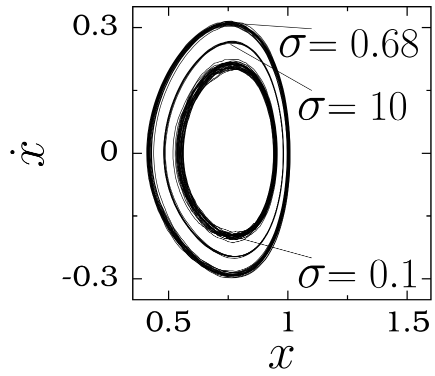

FIG. 9: The phase portrait of the system (2) for three fixed values of σ. Here $\omega = 1$ and $\gamma = 0.4$. Q is maximum at $\sigma = 0.68$.

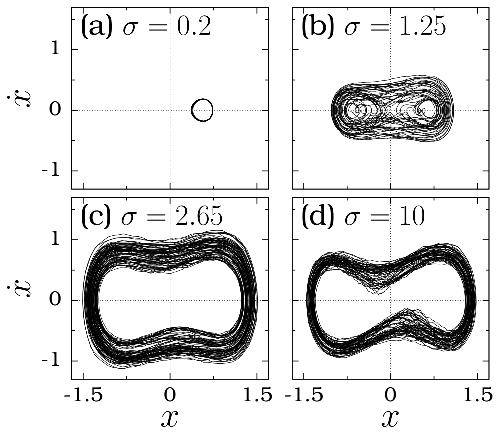

FIG. 10: x versus $\dot{x}$ of the system (2) for $\omega = 1$, $\gamma = 0.65$ and for four fixed values of σ.

and d. The orbit of the system is a cross-well orbit in figs 10b - d, however, Q is maximum for $\sigma = 2.65$. Therefore we can say that $\omega_r = \omega$ at 2.65.

IV CONCLUSION

In the present work we have reported the resonance induced by the random time-delayed feedback in Duffing Oscillator. For small values of ω, the observed resonance is like an additive noise induced stochastic resonance. That is, single resonance occurs and at resonance almost periodic switching between the two wells takes place. For large values of ω double resonance is also realized. At the first resonance cross-well motion is not found to occur.

On the other hand, second resonance takes place far after the cross-well motion.

As the random delay induced resonance in the presence of external periodic force is not strictly like a stochastic resonance. It is important to investigate the occurrence of other types of resonances like coherence, vibrational and ghost resonances in the presence of random delay. Further the study of various resonances with distributive delay, state-dependent delay and time-varying delay can bring out interesting and novel dynamics.

REFERENCES

[1] M Lakshmanan and S Rajasekar, *Nonlinear Dynamics: Integrability, Chaos and Patterns* (Springer, Berlin, 2003).

[2] D W Jordan and P Smith, *Nonlinear ordinary Differential Equations* (Oxford University Press,Oxford, 2007).

[3] A S Pikovsky and J Kurths, *Phys. Rev. Lett.* **78**, 775 (1997).

[4] S Arathi, S Rajasekar and J Kurths, *Int. J. Bifur. & Chaos* **23**, 1350132 (2013).

[5] L Gammaitoni, P Hanggi, P Jung and F Marchesoni, *Rev.Mod. Phys.* **70**, 223 1998.

[6] M D McDonnel, N G Stocks, C E M Pearce and D Abhott, *Stochastic Resonance* (Cambridge Univ. Press, Cambridge, 2008).

[7] D R Chialvo, *Chaos*, **13**, 1226 (2003).

[8] S Rajamani, S Rajasekar and M A F Saujuan, *Commun. Nonlinear Sci.Numer.Simulat.* **19**, 4003 (2014).

[9] P S Landa, P V E McClintock, *J.Phys.A: Math.Gen.* **33**, L433 (2000).

[10] S Jeyakumari, V Chinnathambi, S Rajasekar and M A F Saujuan, *Phys.Rev.E* **80**, 046608 (2009).

[11] S Zambrano, J M Casado, M A F Saujuan, *Phys.Lett.A* **366**, 428 (2007).

[12] M Lakshmanan and D V Senthilkumar, *Dynamics of Nonlinear Time-Delay systems* (Springer, Berlin, 2010).

[13] F M Abay, *Complex Time-Delay Systems: Theory and Applications* (Springer, Berlin, 2010).

[14] J P Finertz, *The population Ecology & cycles in small mammals.* (Yale Univ.Press, New Heaven , 1980).

[15] J R Flowerden, *Mammals: Their Reproductive Biology and Population Ecology* (Edward Arnold, London, 1987).

[16] K I Cooke, Y Kuang and B Li *Can. Appl. Math. Q.* **6**, 321 (1998).

[17] A C Marti, M Ponce and C Masoller, *Phys.Rev.E* **72**, 066217 (2005).

[18] X Liu, S'Zhang and F Zhang, *Chaos, Solitons & Fractals* **24**, 1299 (2005).

[19] D Yue, Y J Zhang, E G Tian, C Perg, *IEEE Trans.Neural Networks* **19**, 1299 (2008).

[20] X Lon, Q Ye and B'Cui, *Neuro computing* **73**, 759 (2010).

[21] S Blythe, X Mao and X Liao, *J.Franklin Inst.* **338**, 481 (2001).

[22] C Massoller and A C Marti, *Phys.Rev.Lett.* **94**, 134102 (2005).

[23] G Wen, G G Wang, C Lin, X Han and G Li, *Chaos, Solitons & Fractals* **29**, 1142 (2006).

[24] Z Wang, F Wang, D W C'Ho and X Liu, *IEEE Trans.Signal Process*, **54**, 2579 (2006).

[25] Z Wang, Y Liu and X Liu, *Automata*, **44**, 1268 (2008).

[26] H Bao and J Cao, *Neural Networks*, **24**, 19 (2011).

[27] T Caraballo, P E Kloeden and J Real, *J. Dyn. Diff. Eqs.*, **18**, 863 (2006).

[28] J Nilsson, B Bernhardsson, S Wittenmark, *Automata*, **34**, 57 (1998).

[29] L M T Romero, B Lindley and I B Schwartz, *Phys.Rev.E*, **86**, 056202 (2012).

[30] Z Sun, X Yang and W Xu, *Phys.Rev.E*, **85**, 061125 (2012).

[31] S L Gao, K Wei, S C Zhong and H Ma, *Phys. Scr.*, **86**, 025002 (2012).

[32] P L Krapivsky, J M Luck and K Mallick, *J.Stat.Mech: Theory and Expt.*, **10**, P10008 (2011).